Luminescence of black phosphorus films: Exfoliation-induced defects and confined excitations

Etienne Carré, Lorenzo Sponza, Alain Lusson, Ingrid Stenger, Sébastien Roux, Frédéric Fossard, Denis Boivin, Nicolas Horezan, Victor Zatko, Pierre Seneor, et al.

Luminescence of Black Phosphorus Films: Exfoliation-induced Defects and Confined Excitations.

Authors

Etienne Carré[1,2*], Lorenzo Sponza[1], Alain Lusson[2], Ingrid Stenger[2], Sébastien Roux[1,2], Frédéric Fossard[1], Denis Boivin[3], Nicolas Horezan[3], Victor Zatko[4], Bruno Dlubak[4], Pierre Seneor[4], Etienne Gaufrès[5], Annick Loiseau[1] and Julien Barjon[2*]

[1] Laboratoire d'Étude des Microstructures (LEM), UMR 104 CNRS-Onera, Université Paris Saclay, 92322 Châtillon, France.
[2] Groupe d'Etude de la Matière Condensée (GEMaC)), CNRS-UVSQ, Université Paris Saclay, 45 Avenue des Etats-Unis 78035 Versailles, France
[3] DMAS, ONERA, Université Paris Saclay, F-92322, Châtillon, France.
[4] Unité Mixte de Physique, CNRS-Thales, Université Paris-Saclay, 91767 Palaiseau, France.
[5] Laboratoire Photonique Numérique et Nanosciences, CNRS-Institut d'Optique-Univ. Bordeaux, 33400 Talence, France

[*]Correspondence: julien.barjon@uvsq.fr, etienne.carre@cnrs-thales.fr

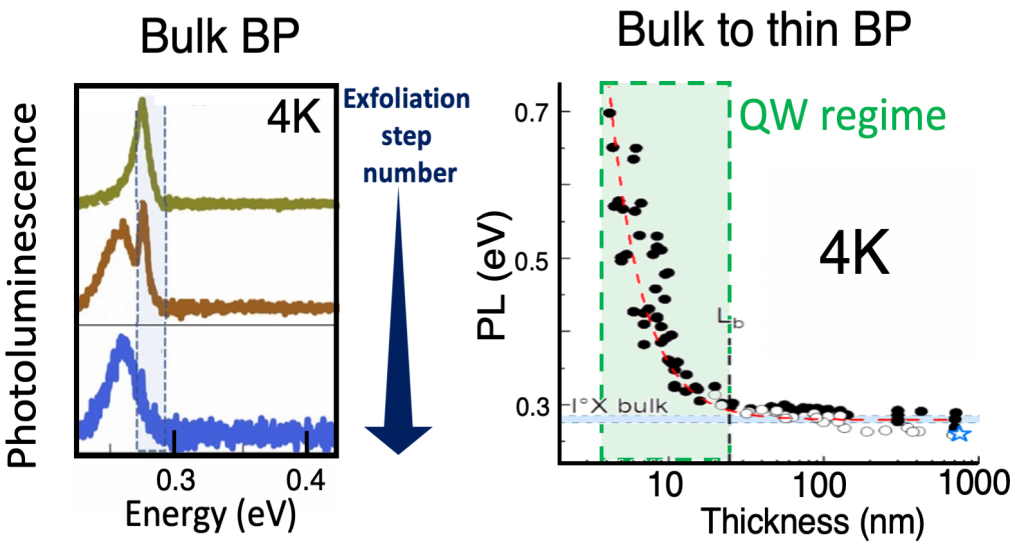

Abstract:

Black phosphorus (BP) stands out from other 2D materials by the wide amplitude of the band-gap energy (ΔE_g) that sweeps an optical window from Visible (VIS) to Infrared (IR) wavelengths, depending on the layer thickness. This singularity made optical and excitonic properties of BP difficult to map. Here we report a comprehensive study of the intrinsic (i.e. measured at 4 K) optical properties of 79 passivated BP flakes obtained by

mechanical exfoliation of thickness ranging from 4 to 700 nm. By following single or multi-stamp exfoliation protocols and by combining micro-Raman and photoluminescence experiments, we demonstrate that the exfoliation step induces line-like defects which open new radiative recombination paths that compete with then replace those of the crystalline bulk. We also show that the evolution of the photoluminescence energy *versus* thickness follows an inverse square law. We relate this to a quantum well model whose validity is discussed and justified at intermediate thickness. Finally, we report that the emission energy of BP slabs placed in different 2D heterostructures is not significantly modulated by the dielectric environment.

Introduction

Confinement effects in 2D materials have attracted considerable interest because of their layered and exfoliable structures that allow angstrom scale increment of the thickness, from monolayer to bulk. Hence, ultrathin layers of 2D semiconductors, such as the MoS_2 and other TDMCs, have demonstrated stunning physical properties, of high significance for optoelectronics and spintronics[1,2]. In this context, black phosphorus (BP), firstly exfoliated in 2014[3,4], stands out from other 2D materials by the peculiar and strong confinement effects on its physical properties. One emblematic feature is the wide amplitude of the band-gap energy (ΔE_g) that sweeps an optical window from Visible (VIS) to Infrared (IR) wavelengths, depending on the number of layers. Indeed, the optical activities in bulk and monolayer BP are centered at 0.3 eV and 2 eV[5], respectively, corresponding to an amplitude energy $\Delta E_{g\text{-}BP} = 1.7\ eV$ considerably wider compared with that observed in the MoS_2 family, roughly $\Delta E_{g\text{-}MoS2} = 0.3\ eV$[6]. Moreover, this variation of $\Delta E_{g\text{-}BP}$ spreads over a large layer number and, for instance, a significant photoluminescence (PL) energy modulation is still observed in the range of 20-30 BP layers.[7]

These singularities make the optical and excitonic properties of BP difficult to map. Specifically, the literature lacks in presenting experimental and theoretical data on the optical properties of BP on an extended thickness range and at cryogenic temperature i.e. below 10K. To be more precise, the large number of works on the subject does cover a large interval of thicknesses, but each single work focuses on a pretty small subset and may differ from the other investigations in many experimental conditions (temperature, exfoliation method, encapsulation, laser power, etc.). These discrepancies do not permit to use them as a consistent ensemble. Moreover, all luminescence measures have been taken at room[8–12] or liquid nitrogen temperature[7,13–15] with the only one exception at cryogenic temperature[16] which actually focuses uniquely on the monolayer. The difficulty to probe BP samples is, furthermore, exacerbated by the poor sensitivity of the detectors in the IR optical range and by the fast and intrinsic photodegradation of BP when placed in ambient conditions.[17,18] The intercrossing of dielectric,

geometrical, defects and mechanical effects with quantum confinement effects also need to be clarified in the ultrathin, thin and bulk-like exfoliated BP flakes. Theoretical[5,19] and experimental[8–10,13,20] studies have been focusing on the behavior of few layers BP emitting in the visible / NIR range. In particular, few works analyzed the strong and anisotropic absorption/emission bands associated to the direct band gap in BP in the 1-4 layers regime[11,13,20]. BP samples were also investigated in the semi-bulk and bulk-like thickness ranges, i.e. arbitrary 4.5 nm to 40 nm[7] and over 400 nm[15]. The study of infrared luminescence of thicker layers of BP has accelerated, partly driven by the emergence of infrared optical applications such as BP based photodetectors and lasing.[7,14,15,21] More recently, the fingerprints of bulk BP PL spectra at 2 K were also reported, showing the existence of free and bound excitons energy around a refined value of the bandgap of 0.287 eV at cryogenic temperature[22].

Here we report on an unprecedented ensemble of cryogenic temperature (4 K) PL spectra from 79 passivated BP flakes with thicknesses ranging from 4 nm to 700 nm, obtained by mechanical exfoliation. In the first part of this article, we crosslink micro-Raman data with photoluminescence spectra and optical images to highlight a correlation between exfoliation-induced defects and a low-energy broad band (defect band) in the PL spectra. Hence we demonstrate that the nature of the emission in exfoliated BP flakes is dominated by defect states that compete with the radiative recombination of bound excitons observed in as-grown crystals. In the second part of the article, we focus on the evolution of the PL peak as a function of the thickness finding that our data can be explained with a quantum well model and we discuss its limits of validity. We also show that the dielectric environment does not modulate the photoluminescence energy from BP layers sandwiched in different 2D heterostructures. Finally, we rationalize these results arguing that it is the confinement of the wavefunction of the excitation that causes the modulation of the signal with the thickness, and not the variation of the interaction between the excited particles.

Main text

Defect-related emission from exfoliated crystals.

The BP crystals were purchased from HQ Graphene and were mechanically exfoliated by an usual repeatable stamping process in a glovebox under argon atmosphere (<0.5 ppm O_2, <1 ppm H_2O) to prevent BP degradation. The thickness of the flakes was characterized by combining optical and Atomic Force Microscopy (AFM), both installed in the glovebox. A custom-built transfer box was used to transfer the samples into an Atomic Layer Deposition (ALD) chamber to perform a homogeneous deposition of a 10 nm Al_2O_3 passivation

layer. Further details on the sample preparation and PL characterization can be found in the supplementary information file SupMat1).

In Figure 1 we compare representative photoluminescence spectra recorded at 4 K with an inversed FTIR microscope from: an as-received BP crystal (1a); a crystal resulting from a single-stamping exfoliation deposited on a Si/SiO_2 substrate (1b); and a thick BP flake (700 nm) obtained from a multiple-stamping exfoliation deposited on substrate (1c). The corresponding photography and optical images are shown in Figure 1d. As described in[22], the PL of the as-received crystal consists of two structures. A fine emission signal is formed mainly of free and bound excitons (I°X) lines, and is highlighted by the pale-blue strip in the Figure 1a-c. A second contribution at about 20 meV lower energy is related to defect-assisted recombination. Because size effects are negligible at this thickness, as we will demonstrate below, the PL fingerprints are expected to look similar in all three samples. Surprisingly, even if the overall PL emission bands fall in the same tight energy interval (50 meV), the line shape is significantly modified. The excitonic fine structure of BP crystal (sharp peak) clearly disappeared leaving a broadened emission line for the sample obtained via multiple-stamping exfoliation (Figure 1c). The characteristics of this emission peak (line widths ranging from 15 meV to 45 meV) are consistent with the PL spectra reported in the literature for different thick flakes obtained via mechanical exfoliation[7,14,15,21].

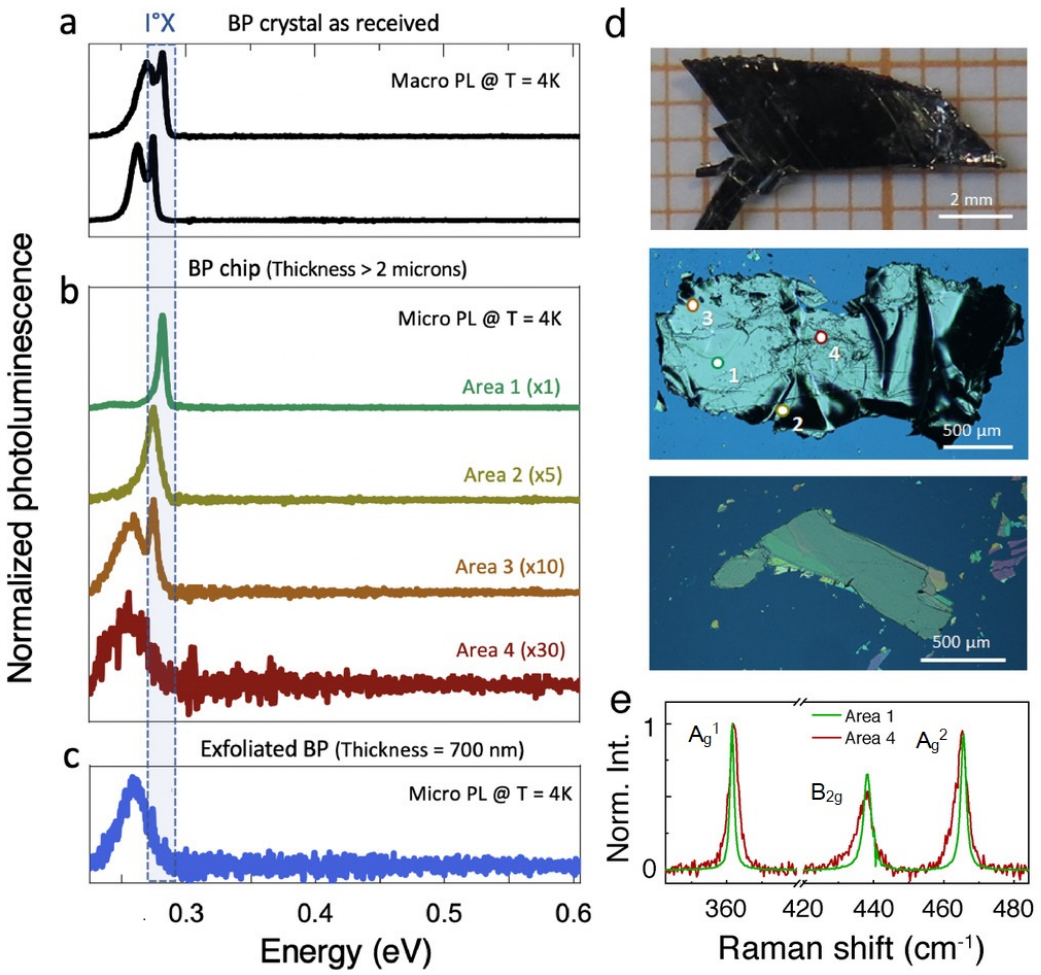

Figure 1. Photoluminescence spectra recorded a 4 K from **(a)** an as-received BP crystal, **(b)** from a thick BP chip obtained after a single-stamping exfoliation step, and **(c)** from a 700 nm thick flake obtained after multiple-stamping exfoliation steps. The excitation wavelength is 532 nm and the fluence is 2.10^2 W.cm^{-2} for the macro-PL (a) and 3.10^3 W.cm^{-2} for the micro-PL (b,c) experiments. **(d)** Photography and optical images corresponding to the three samples analysed in (a,b,c) from top to bottom. Labels 1 to 4 refer to the areas where spectra in (b) are recorded. **(e)** Raman spectra recorded from areas 1 and 4 of the sample (b) with a 633 nm excitation laser.

To investigate these characteristics in more detail, we operated a single-stamping exfoliation of a BP crystal, i.e. we stamped the crystal with PDMS only once, hence obtaining a BP chip of micron scale thickness, corresponding to an intermediate thickness sample ranging between the size of the BP crystal and the ultrathin samples commonly reported in literature. Low temperature micro-PL spectra recorded at different selected areas of this BP chip (areas labeled 1 to 4 in the image of the sample in Figure 1d) interestingly exhibit different PL line shapes (Figure 1b). We observe that a bright and narrow band dominates the emission fingerprint for areas 1 and 2. The emission energy and linewidth present strong similarities with those of the I°X bound exciton found in the pristine crystal[22]. On the other hand, the area 4 displays a broad emission band centered at lower energy, similar to the low-energy emission band of the BP crystal reported by some of us[22]. An intermediate situation with the coexistence of the two

bands is observed in some regions of the chip, alike area 3. They reproduce the overall macro PL spectrum recorded on the crystal.

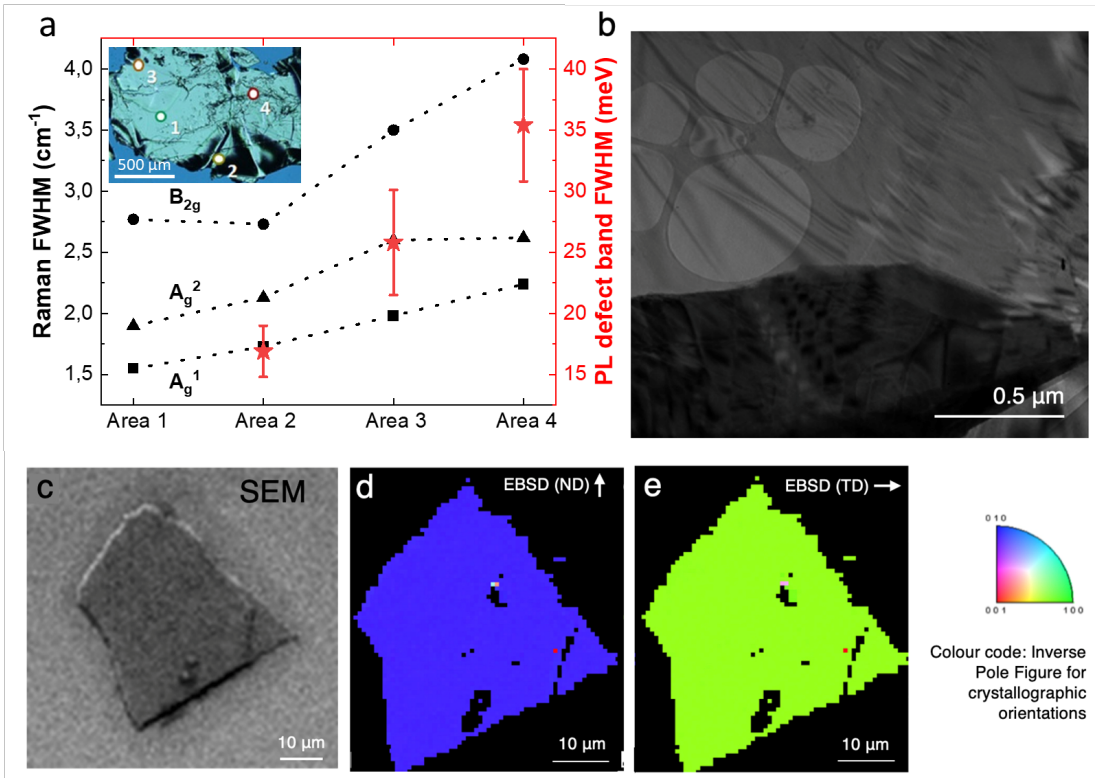

Figure 2. **(a)** Full Width at Mid-Height of the Raman modes (A_g^1, B_{2g} and A_g^2 in black) and of the defect related PL peak (in red) as a function of the area analyzed. Inset : Optical image of the multi-exfoliated flake presented in Figure 1d. **(b)** HRTEM image at 200 kV of a multi-exfoliated BP flake. **(c)** SEM image of a multi-exfoliated BP flake and its corresponding EBSD maps parallel to the normal **(d)** and transverse **(e)** axes.

Qualitative observation from the optical image, combined with statistical measurements of the FWHM of the A_g^1, B_{2g} and A_g^2 Raman modes indicates a decreasing crystal quality from area 1 to area 4 (Figure 1e). By crosslinking data from micro-Raman and PL (see Figure 2a), it appeared clearly that this broadening of the Raman modes is strongly correlated with the emergence and the broadening of a strong PL emission band at lower energy with respect to the intrinsic I°X emission band (see details in SupMat 2). This means that PL from Area 1 and 2 come from low-defective zones of the BP sample where the radiative pathway is driven by bound excitons, whereas light emission from the other zones is more or less dominated by defects, depending on their density. It can be noticed that after a multistamping process, the intrinsic I°X band completely vanishes and most of the PL originates from the defect band.

While it can firmly asserted that these defects are actually generated by the exfoliation process itself, it remains difficult to discriminate the origin of the defects and several hypothesis can be screened.

Vacancies present in BP have been shown to play the role as acceptor defects[23,24], and may be the cause of the I^0X peak.[22] However, the generation of such vacancies, as the emergence of interstitial atoms or substitution atoms seems unlikely during exfoliation. The hypothesis of stacking defects deserves more attention as exfoliation may lead to twisted BP stacks. However, EBSD measurements carried out on exfoliated BP flakes (Figure 2c to 2e) show a single distribution of crystal orientations on the whole thickness of the flake. The absence of twisted BP planes enable us to rule out exfoliation-generated misorientations of the BP layers in a given flake.

Figure 2b shows typical HAADF-TEM images recorded from a multistamped exfoliated BP flake. It clearly appears that the material have undergone plastic deformation due to the stress caused by exfoliation. Similar features have been already reported in exfoliated MoS_2 or hBN, where an equivalent broadening of the PL band is observed[25,26] and attributed to exfoliation induced linear defect type.[27,28]

In light of these observations, we conclude that the exfoliation based on PDMS stamping, commonly used for producing BP samples, introduces linear defects of some kind that induce deep changes in the nature of the luminescent process in BP layers, resulting in a broad emission band that may rely to the low-energy band observed in the pristine crystal in macro PL. This phenomenon is not specific to BP, but may be favored by its puckered structure.

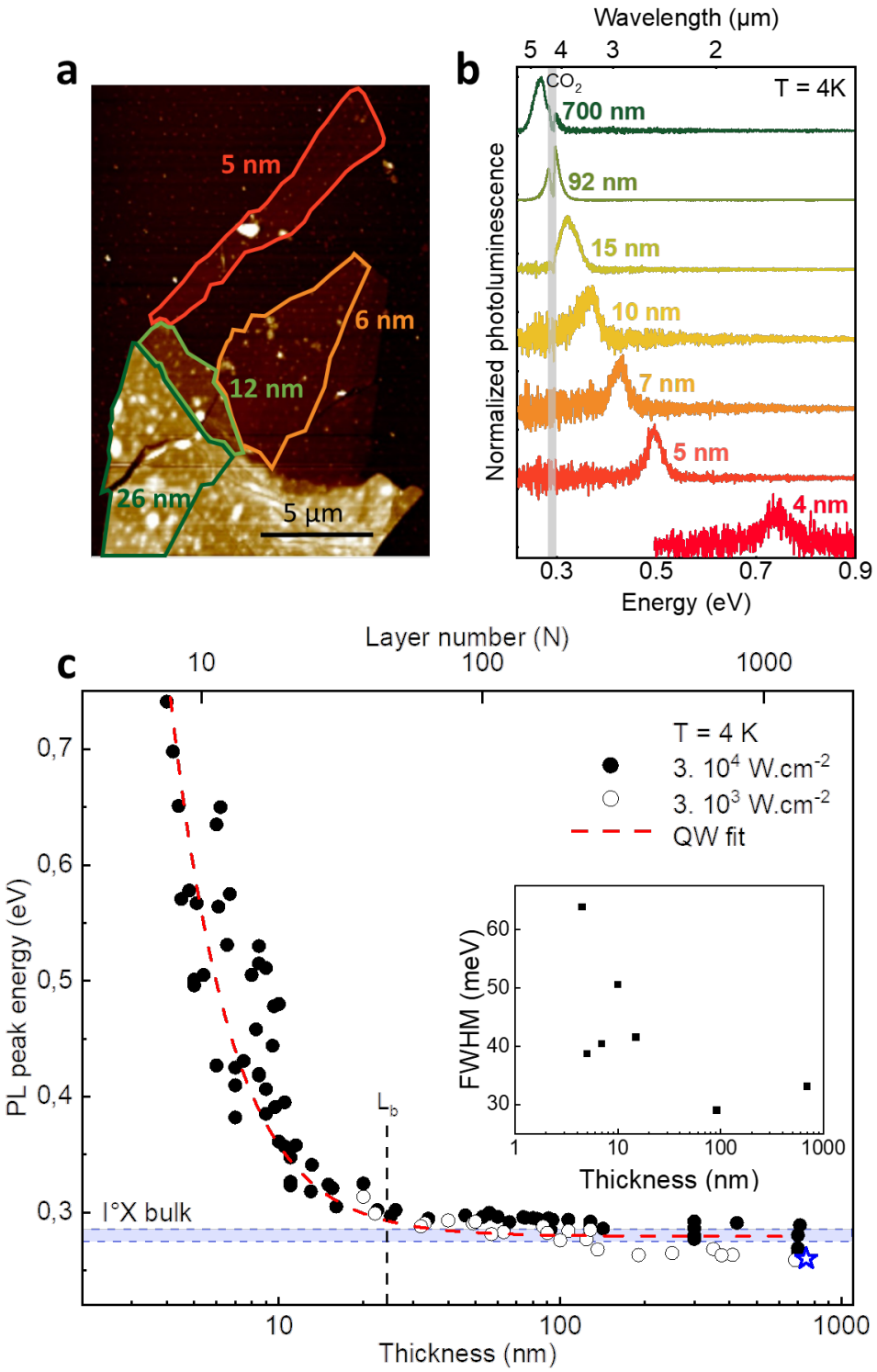

Figure 3 (**a**) Representative AFM image of exfoliated BP and deposited on Si/SiO_2. (**b**) Selection of photoluminescence spectra of BP flakes at different thicknesses probed at 4 K and excited at a wavelength of 532 nm and at a fluence of 3.10^4 W.cm^{-2}. The grey line indicates the part of the spectra disturbed by the CO_2 absorption band. (**c**) Evolution of the PL peak energy as a function of the thickness (black bullets and circles) and its fit based on a quantum well (QW) model. (red dashed line). The bound exciton energy of the BP crystal at 4 K is marked as a horizontal blue line. A black dashed line indicates the threshold thickness at 25 nm. The blue star corresponds to the energy of the PL peak shown in Figure 1c. Inset: FWHM of the PL a of Figure 3b as a function of the thickness.

Quantum-confinement on a large thickness range

To further investigate the characteristics of the emission peak, we probed the photoluminescence of 79 BP exfoliated flakes at 4K, with thickness ranging from 4 nm to 700 nm (see SupMat1 in the supplementary information file for details on PL measurements procedure). The AFM image of a representative thin sample is displayed in Figure 3a whereas a set of optical and AFM images of other flakes are presented in SupMat3. Figure 3b presents the normalized PL spectra at cryogenic temperature of typical BP flakes. The grey line indicates the part of the spectra disturbed by the CO_2 absorption band coming from the free-space part of the collection beam in our apparatus. In all exfoliated samples we probed, the luminescence spectra consist in a single and broadened emission band with a line width ranging from 25 meV to 60 meV. There is a tendency for the width of the luminescence band at half-height to increase as thickness decreases (see inset of Figure 3c), although clearer differences can be seen between flakes of the same thickness but differing in quality/homogeneity. More generally, the half-height width of luminescence at 4K is of the same order of magnitude as that at 80K (see SupMat4) and even at higher temperature in the literature[15]. This temperature independence is a further confirmation of the fact that, contrary to what is observed in other 2D materials (e.g. in TMDs[29]), the broadening is not related to size-effects on the intrinsic emission of the material, but it is dominated by defects introduced by the very exfoliation as illustrated in the previous section. Note that the PL band from the thickest flakes coincides with the broadened band reported in Figure 1c. Even if a single broad PL band is observed in all samples and at all thicknesses, and even if the luminescence is linked to defects in the bulk BP, we can not exclude that the nature of the emission changes drastically at atomic thickness (monolayer or very few layers). For each flake, we associate the energy of the emission to the maximum of the PL spectrum. When it falls in the CO_2 absorption range (gray rectangle in Figure 3b), for example for the 92 nm film, the PL signal is modeled with a Gaussian peak and the energy at maximum is extrapolated.

The evolution of the PL peak energy from about 10 to about 1000 layers follows two distinct regimes with a transition thickness (L_b) around 25 nm (about 50 layers), as highlighted by a black dashed line in Figure 3c, and as can be observed also in the data published by Chen et coworkers[7].

At thicknesses higher than L_b, the PL energy evolves moderately, from 0.27 eV to 0.32 eV, and remains close to that of the bound exciton (0.275 eV at 2 K,blue star in Figure 3c). These values are, in average, slightly lower than those presented in the literature for the same thickness range (0.32 eV[21] and 0.31 eV[15] for 70 nm and 220 nm-thick BP layers probed at 80 K, respectively) but this can be explained by the fact that the gap of black phosphorus blueshifts with temperature[30,31]. Measures have been taken at two different excitation fluences: black bullets

and empty circles correspond to laser powers of $3x10^4$ and $3x10^3$ $W \cdot cm^{-2}$, respectively. No degradation was observed under exposure, i.e. no trace of the laser spot under the microscope and no decrease of the luminescence signal over time. We only notice a weak dependence of the peak energy on the excitation fluence of the order of few tens of meV, which could be ascribed to the Burstein Moss effect[32,33] (more details in SupMat5).

At thicknesses lower than L_b, the peak energy increases significantly, reaching 0.7 eV for the 4 nm-thick BP flake. For comparison, our seven thinnest flakes (4.0 to 5.0 nm) have an emission peak comprised between 0.7 and 0.5 eV, with 0.57 eV for the 4.5 nm-thick one. Chen and coworkers[7] measured only one sample in this range with an emission of 0.45 eV and a thickness of 4.5 nm. Their measure is quite comparable with ours even though a bit lower. Burstein Moss and temperature effects may explain some tens of meV discrepancy, but a more relevant parameter to be considered is the size of the probe spot, which can range from several microns (Our work, Chen *et al.*[7]) to a hundred[15]. Ultra-thin exfoliated BP samples are seldom homogeneous on a micrometer scale, so it is hard to relate a PL spectrum to a narrow thickness estimation. Here, we would like to stop and stress a point valid for 2D materials in general, and for BP in particular. At small thickness, it is barely meaningful to compare single PL spectra as uncertainties in the thickness (e.g. due to large spot size and low homogeneity) may lead to large errors. Instead, a more statistical approach should be preferred.

We observe that the evolution of the experimental peak energies as a function of the thickness can be well described by the law $E = \frac{\hbar^2\pi^2}{2m^*L^2} + E_0$, where E_0 is an offset energy and L is the thickness of the slab. We fixed the value of $E_0 = 0.279$ eV to the average energy of PL measurements on the 700 nm thick flake and since we measured the thickness, we could fit the model with only one parameter: the effective mass, getting $m^*=0.049m_0$ (m_0: mass of the electron in vacuum). This inverse quadratic law can be derived from a two-particle quantum well model (SupMat6) where two non-interacting charges are free to move in a continuous medium under the confining action of infinite potential barriers. We think that this model, despite its simplicity, can be safely applied to describe the emission from BP slabs at the condition of interpreting m* as an electron-hole pair effective mass modified by the defects introduced by the exfoliation. We recall in fact that BP has unique characteristics among the 2D family (cfr Figure 4c) because excitations widely spread among the layers[22] and charges do not localize on individual planes[22,34]. Therefore, in thick enough slabs (approximately above 10 layers), the hypotheses behind the model are met (insensitivity to the layered structure, negligible wavefunction spill-out and weak electron-hole interactions) so it is pertinent even if we are in presence of van der Waals interactions instead of covalent bondings. On the other hand, when the slab is thinned too much, it is sensible to think that one or more of the approximations above break down and different models shall be preferred, similarly to what

observed in small-size Si nanostructures[35–37]. Examples of models introduced for the ultra-thin BP slabs are different power laws[5,9,38], or the tight-binding model introduced by Zhang and coworkers[7,12,13,39,40] which treats explicitly the interlayer hopping and whose large thickness limit is precisely the quantum well model, as demonstrated analytically and numerically by its authors for slabs of 13 and 15 layers.

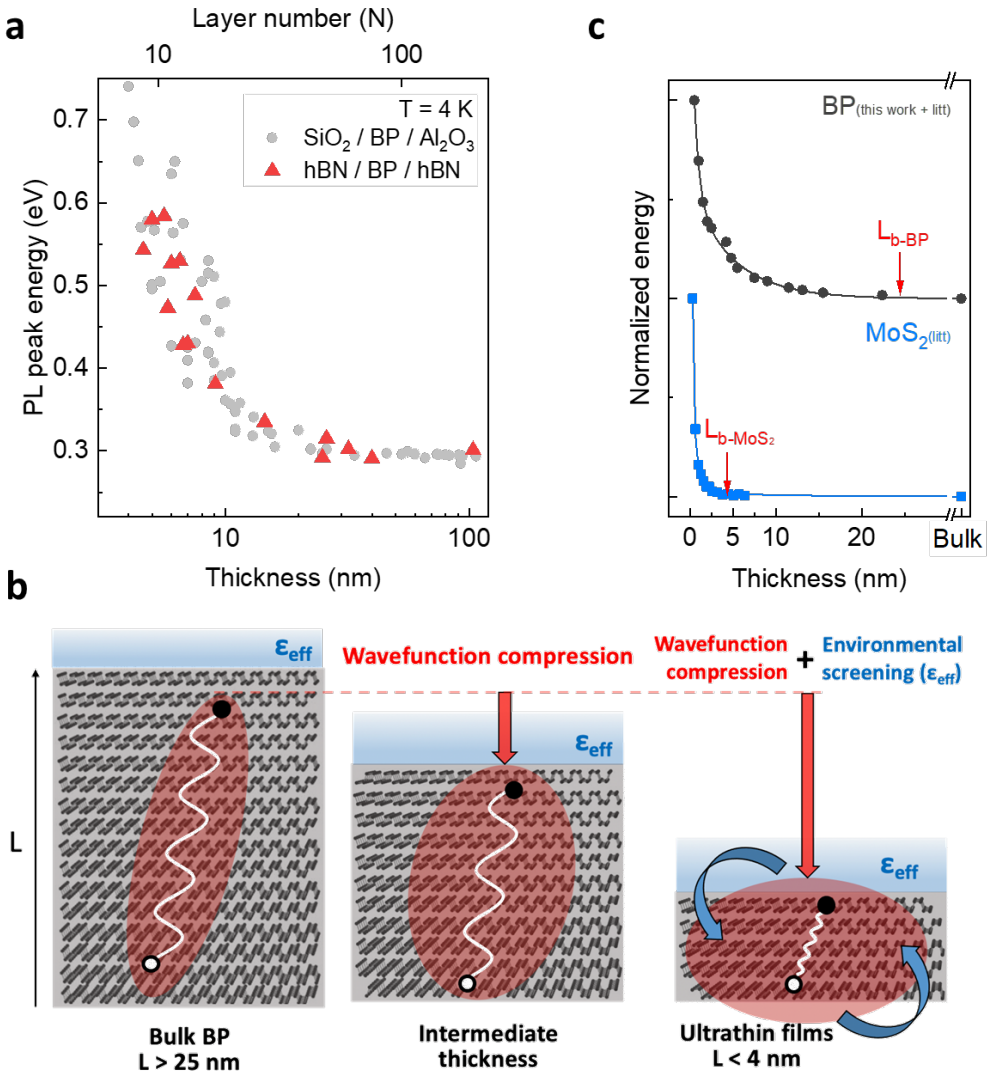

Figure 4. (**a**) Variation of the photoluminescence peak energy with the thickness. hBN / BP / hBN (red triangles) and SiO_2/BP/Al_2O_3 (gray dots) heterostructures. (**b**) Schematic of the BP excitation for a thick, intermediate and an ultrathin sample reading from left to right. In the intermediate regime, only the effect of the compression of the wave function is observed. The environmental screening appears at lower thickness[20] as well as the sensitivity to the layered structure. (**c**) Comparison of the band energy variation in BP and MoS_2[6,41,42]. Red arrows indicate the limit beyond which the energy band gap varies by approximately 1% of the total band gap modulation from the monolayer to the bulk.

To test if the evolution in this intermediate thickness range is altered by the dielectric environment, as it is often put forward in ultra-thin films[20,43–47], we compared the evolution of the photoluminescence energy of some hBN / BP / hBN heterostructures (hBN has a dielectric

constant of about 3[48]) with the SiO_2/BP/Al_2O_3 samples studied above (the dielectric constant of alumina is around 9[49]). More details on the heterostructures fabrication and their luminescence are given in the SupMat7. Results are reported in Figure 4a in red triangles (hBN encapsulated) and grey bullets (alumina-passivated samples of Figure 3). The superposition of the PL energy as a function of thickness demonstrate that the emission is not significantly affected by changes of the dielectric environment, at least in this range of thickness.

These two points (the quantum well fit and the insensitivity to the dielectric environment) suggest a consistent picture of the effects of confinement on the emission of BP films. The excitation occurring in PL is a neutral excitation involving particles of different charges which emit back upon relaxation. In the following we will use the term particle-hole pair in this wide sense, regardless its free or bound nature. In this context, it is still sensible to use the reduced-mass model we introduced in[22] and solve it for an excitation with the fitted effective mass 0.049 m_0. We calculated the extension of the excitation in 3D as detailed in the SupMat8, and we found that 90% of the excitation occupies a slab 28.8 nm thick, to be compared with 6.5 nm for MoS_2. In the reduced-mass model, size effects may occur because of two reasons: a compression of the wavefunction of the excitation and/or a modification of the interaction between the particles involved (for instance because of changes in the dielectric environment as in the Rytova-Keldysh potential[50,51]). The first effect impacts mostly the kinetic part of the pair and only if the layered-nature of the structure can be disregarded (continuous material). Its variation goes as $1/L^2$ if the confining potential can be well approximated by infinite barriers (negligible wavefunction spill-out). The second effect impacts only the interacting term. Given the extension of the excitation, we argue that in the intermediate thickness range the variation of the PL energy are due uniquely to the confinement of the wavefunction by infinite barriers, because the films are too thick for the environmental screening to play a role, for the layered structure to impact the excitation and for the wavefunction to spill-out. We made a sketch of this interpretation in Figure 4b. We are supported in this interpretation by four clues. The first is the insensitivity of our measurements to the dielectric environment. The second is that in the derivation of the quantum well model (cfr. SupMat6) there is no interaction term (independent particle approximation). The third is that the experimental trend is correctly $1/L^2$ (infinite potential barriers). The fourth is that the wavefunction extension of our 3D reduced mass model predicts reasonably well the thickness at which the wavefunction should start "feeling" the compression (25 nm in BP, ~4.5 nm in MoS_2, cfr. Figure 4c).

Our interpretation allows us to identify the limits of applicability of the quantum well model and relate them to the physics of the confined excitation. At large thickness, the model ceases to be relevant when the thickness is larger than the extension of the excitation, limit that we

measure at about 25 nm and we explain theoretically. At small thickness, we have not been able to observe experimentally the limit, but it should be around 10 layers[39]. Around this thickness, besides the extreme compression of the wavefunction that breaks down the infinite barrier approximation, the excitation should start being impacted by the layered nature of the material (discrete material) and the interaction between the particles should start being modified by the environmental screening, as in the Rytova-Keldysh potential. Then the quantum well (non-interacting) model ceases to be valid and other models becomes more relevant[5,7,9,12,13,38–40].

Finally let us stress the unicity of these characteristics among the 2D family and their potential for technological applications. The quantum well regime is observable already at moderate thickness (below 25 nm, i.e. below about 50 layers) and the increase of the peak energy is quite slow as attested by the very low effective mass of the model ($m^*=0.049m_0$). For a comparison, in MoS_2 the PL energy enters a quantum well regime at about 5 layers (L_b=2-3 nm) and increases steeply (see Figure 4c). This slow change of the PL energy may be an advantage for possible applications because it makes the modulation of the emission easier to control. Furthermore, we observed that these characteristics are robust against changes of the substrate or the passivation layer, which may be another advantage as it simplifies the integration of BP slabs in actual devices.

Conclusions

To conclude, our work reports on two characteristics related closely to the unique mechanical and electronic properties of BP.

Thanks to a micro-PL analysis of single-stamp exfoliated samples, we demonstrate that the shape of the emission peak is modified by the exfoliation process itself because it introduces some structural disorder or defects that alter the recombination pathways of the excitation. The resulting peak coincides at very large thickness with the low-energy band of the bulk crystal spectrum. We ascribe this exceptional sensitivity of the PL signal to the exfoliation process to the high softness of BP which is a unique characteristics in the 2D family.

We report also on the evolution of luminescence at cryogenic temperature of many exfoliated slabs of black phosphorus over a wide and so far unexplored range of thicknesses under two different dielectric environments. These measures permitted us to get a consistent overview on the intrinsic signal of BP film and gain insight into the confinement of the excitation. We show that a quantum well model describes well the evolution of the PL energy as a function of the film thickness and we highlight its limits of applicability. By means of a 3D reduced-mass model, we rationalize the evolution of the signal as a consequence of the compression of the

excitation wavefunction and we are able to explain why our measures are insensitive to changes of the dielectric environment. We identify in the low effective mass of the particles involved in the excitation the connection between the peculiar electronic structure of BP and the wide range of applicability of the quantum well regime.

Acknowledgments.

The authors acknowledge funding from the French national research agency (ANR) under the grant agreement No. ANR-17-CE24-0023-01 (EPOS-BP). This project has also received funding from the European Union's Horizon 2020 research and innovation program under grant agreement N° 881603 (Graphene Flagship core 3).

References:

1. Cheng, J., Wang, C., Zou, X. & Liao, L. Recent Advances in Optoelectronic Devices Based on 2D Materials and Their Heterostructures. *Advanced Optical Materials* **7**, 1800441 (2019).
2. Han, W. Perspectives for spintronics in 2D materials. *APL Materials* **4**, 032401 (2016).
3. Xia, F., Wang, H. & Jia, Y. Rediscovering black phosphorus as an anisotropic layered material for optoelectronics and electronics. *Nat Commun* **5**, 4458 (2014).
4. Li, L. *et al.* Black phosphorus field-effect transistors. *Nature Nanotech* **9**, 372–377 (2014).
5. Tran, V., Soklaski, R., Liang, Y. & Yang, L. Layer-controlled band gap and anisotropic excitons in few-layer black phosphorus. *Phys. Rev. B* **89**, 235319 (2014).
6. Mak, K. F., Lee, C., Hone, J., Shan, J. & Heinz, T. F. Atomically Thin MoS 2 : A New Direct-Gap Semiconductor. *Phys. Rev. Lett.* **105**, 136805 (2010).
7. Chen, C. *et al.* Bright Mid-Infrared Photoluminescence from Thin-Film Black Phosphorus. *Nano Lett.* **19**, 1488–1493 (2019).
8. Pei, J. *et al.* Producing air-stable monolayers of phosphorene and their defect engineering. *Nat Commun* **7**, 10450 (2016).

9. Yang, J. *et al.* Optical tuning of exciton and trion emissions in monolayer phosphorene. *Light Sci Appl* **4**, e312–e312 (2015).
10. Zhang, S. *et al.* Extraordinary Photoluminescence and Strong Temperature/Angle-Dependent Raman Responses in Few-Layer Phosphorene. *ACS Nano* **8**, 9590–9596 (2014).
11. Wang, X. *et al.* Highly anisotropic and robust excitons in monolayer black phosphorus. *Nature Nanotech* **10**, 517–521 (2015).
12. Wang, F. *et al.* Electronic structures of air-exposed few-layer black phosphorus by optical spectroscopy. *Phys. Rev. B* **99**, 075427 (2019).
13. Li, L. *et al.* Direct observation of the layer-dependent electronic structure in phosphorene. *Nature Nanotech* **12**, 21–25 (2017).
14. Chen, C. *et al.* Widely tunable mid-infrared light emission in thin-film black phosphorus. *Sci. Adv.* **6**, eaay6134 (2020).
15. Zhang, Y. *et al.* Wavelength-Tunable Mid-Infrared Lasing from Black Phosphorus Nanosheets. *Adv. Mater.* **32**, 1808319 (2020).
16. Surrente, A. *et al.* Excitons in atomically thin black phosphorus. *Phys. Rev. B* **93**, 121405 (2016).
17. Favron, A. *et al.* Photooxidation and quantum confinement effects in exfoliated black phosphorus. *Nature Mater* **14**, 826–832 (2015).
18. Island, J. O., Steele, G. A., van der Zant, H. S. J. & Castellanos-Gomez, A. Environmental instability of few-layer black phosphorus. *2D Mater.* **2**, 011002 (2015).
19. Qiao, J., Kong, X., Hu, Z.-X., Yang, F. & Ji, W. High-mobility transport anisotropy and linear dichroism in few-layer black phosphorus. *Nat Commun* **5**, 4475 (2014).
20. Gaufrès, E. *et al.* Momentum-Resolved Dielectric Response of Free-Standing Mono-, Bi-, and Trilayer Black Phosphorus. *Nano Lett.* **19**, 8303–8310 (2019).
21. Wang, J. *et al.* Mid-infrared Polarized Emission from Black Phosphorus Light-Emitting Diodes. *Nano Lett.* **20**, 3651–3655 (2020).

22. Carré, E. *et al.* Excitons in bulk black phosphorus evidenced by photoluminescence at low temperature. *2D Mater.* **8**, 021001 (2021).
23. Kiraly, B., Hauptmann, N., Rudenko, A. N., Katsnelson, M. I. & Khajetoorians, A. A. Probing Single Vacancies in Black Phosphorus at the Atomic Level. *Nano Lett.* **17**, 3607–3612 (2017).
24. Guo, Y. & Robertson, J. Vacancy and Doping States in Monolayer and bulk Black Phosphorus. *Sci Rep* **5**, 14165 (2015).
25. Ciampalini, G. *et al.* Light emission properties of mechanical exfoliation induced extended defects in hexagonal boron nitride flakes. *2D Mater.* **9**, 035018 (2022).
26. Van Der Zande, A. M. *et al.* Grains and grain boundaries in highly crystalline monolayer molybdenum disulphide. *Nature Mater* **12**, 554–561 (2013).
27. Watanabe, K., Taniguchi, T., Kuroda, T. & Kanda, H. Band-edge luminescence of deformed hexagonal boron nitride single crystals. *Diamond and Related Materials* **15**, 1891–1893 (2006).
28. Bourrellier, R. *et al.* Nanometric Resolved Luminescence in h-BN Flakes: Excitons and Stacking Order. *ACS Photonics* **1**, 857–862 (2014).
29. Cadiz, F. *et al.* Excitonic Linewidth Approaching the Homogeneous Limit in MoS 2 - Based van der Waals Heterostructures. *Phys. Rev. X* **7**, 021026 (2017).
30. Villegas, C. E. P., Rocha, A. R. & Marini, A. Anomalous temperature dependence of the band-gap in Black Phosphorus. *Nano Lett.* **16**, 5095–5101 (2016).
31. Baba, M., Nakamura, Y., Shibata, K. & Morita, A. Photoconduction of Black Phosphorus in the Infrared Region. *Jpn. J. Appl. Phys.* **30**, L1178–L1181 (1991).
32. Burstein, E. Anomalous Optical Absorption Limit in InSb. *Phys. Rev.* **93**, 632–633 (1954).
33. Moss, T. S. The Interpretation of the Properties of Indium Antimonide. *Proc. Phys. Soc. B* **67**, 775–782 (1954).
34. Low, T. *et al.* Tunable optical properties of multilayer black phosphorus thin films. *Phys. Rev. B* **90**, 075434 (2014).

35. Delley, B. & Steigmeier, E. F. Size dependence of band gaps in silicon nanostructures. *Applied Physics Letters* **67**, 2370–2372 (1995).
36. Read, A. J. *et al.* First-principles calculations of the electronic properties of silicon quantum wires. *Phys. Rev. Lett.* **69**, 1232–1235 (1992).
37. Barbagiovanni, E. G., Lockwood, D. J., Simpson, P. J. & Goncharova, L. V. Quantum confinement in Si and Ge nanostructures: Theory and experiment. *Applied Physics Reviews* **1**, 011302 (2014).
38. Tran, V., Fei, R. & Yang, L. Quasiparticle energies, excitons, and optical spectra of few-layer black phosphorus. *2D Mater.* **2**, 044014 (2015).
39. Zhang, G. *et al.* Infrared fingerprints of few-layer black phosphorus. *Nat Commun* **8**, 14071 (2017).
40. Huang, S. *et al.* From Anomalous to Normal: Temperature Dependence of the Band Gap in Two-Dimensional Black Phosphorus. *Phys. Rev. Lett.* **125**, 156802 (2020).
41. Zhao, Z.-Y. & Liu, Q.-L. Study of the layer-dependent properties of MoS_2 nanosheets with different crystal structures by DFT calculations. *Catal. Sci. Technol.* **8**, 1867–1879 (2018).
42. Gołasa, K. *et al.* Optical Properties of Molybdenum Disulfide (MoS_2). *Acta Phys. Pol. A* **124**, 849–851 (2013).
43. Qiu, D. Y., da Jornada, F. H. & Louie, S. G. Environmental Screening Effects in 2D Materials: Renormalization of the Bandgap, Electronic Structure, and Optical Spectra of Few-Layer Black Phosphorus. *Nano Lett.* **17**, 4706–4712 (2017).
44. Bradley, A. J. *et al.* Probing the Role of Interlayer Coupling and Coulomb Interactions on Electronic Structure in Few-Layer $MoSe_2$ Nanostructures. *Nano Lett.* **15**, 2594–2599 (2015).
45. Latini, S., Olsen, T. & Thygesen, K. S. Excitons in van der Waals heterostructures: The important role of dielectric screening. *Phys. Rev. B* **92**, 245123 (2015).
46. Andersen, K., Latini, S. & Thygesen, K. S. Dielectric Genome of van der Waals Heterostructures. *Nano Lett.* **15**, 4616–4621 (2015).

47. Chernikov, A. *et al.* Exciton Binding Energy and Nonhydrogenic Rydberg Series in Monolayer WS 2. *Phys. Rev. Lett.* **113**, 076802 (2014).
48. Laturia, A., Van de Put, M. L. & Vandenberghe, W. G. Dielectric properties of hexagonal boron nitride and transition metal dichalcogenides: from monolayer to bulk. *npj 2D Mater Appl* **2**, 6 (2018).
49. Vila, R., González, M., Mollá, J. & Ibarra, A. Dielectric spectroscopy of alumina ceramics over a wide frequency range. *Journal of Nuclear Materials* **253**, 141–148 (1998).
50. Rytova, N. S. Screened potential of a point charge in a thin film. *Proc. MSU, Phys., Astron.* **3**, (1967).
51. Keldysh, L. V. Coulomb interaction in thin semiconductor and semimetal films. *JETP Lett.* **29**, 658–661 (1979).